

Information-theoretic characterization of turbulence intermittency

Shreyashri Sarkar and Rishita Das*

Department of Aerospace Engineering, Indian Institute of Science, Bangalore, KA, India

(Dated: May 9, 2025)

We present a new characterization of small-scale intermittency of turbulence based on an information-theoretic measure, that inherently segregates turbulence intermittency from kinematic intermittency. Instead of the commonly studied higher-order moments, Kullback-Leibler (KL) divergence is used to quantify the deviation of turbulence pseudodissipation rate (or dissipation rate/enstrophy) from that of a Gaussian random velocity field as an accurate measure of the small-scale intermittency arising from turbulence dynamics. In addition, Shannon entropy is used to assess the uncertainty of these turbulence small-scale quantities. Analysis of direct numerical simulation data of forced homogeneous isotropic turbulent flow reveals the existence of two critical Taylor Reynolds numbers where the variation of uncertainty changes. The KL-divergence measure reveals two striking results about intermittency: (i) intermittency grows logarithmically with Reynolds number and (ii) dissipation rate and enstrophy are equally intermittent in a turbulent flow of any Reynolds number, if one considers only the intermittency arising from turbulence dynamics.

The irregular and sporadic spatio-temporal occurrence of extreme velocity gradients in a turbulent flow manifests as a specific non-Gaussian behavior that is referred to as small-scale intermittency [1–4]. To measure this intermittency, researchers have typically relied on higher order moments, such as kurtosis (fourth order moment), of dissipation rate and other velocity gradient quantities [5–10]. Based on moments, Yakhot and Donzis [11, 12] and Schumacher et al. [13] have demonstrated the transition of velocity gradients from Gaussian to non-Gaussian statistics at a critical Taylor Reynolds number $Re_\lambda \sim 10$ ($Re_\lambda \equiv u_{rms}\lambda/\nu$, where λ is Taylor micro-scale, u_{rms} is root mean square of velocity fluctuations, and ν is kinematic viscosity). Above the transitional Reynolds number, moments grow as power laws of Re_λ , with different scaling exponents for different moment orders. However, individual moments do not specify the complete probability density function (PDF), resulting in a somewhat ambiguous quantification of intermittency based on the specific order moment one chooses to evaluate. Additionally, the estimation of higher order moments is extremely sensitive to rare events and requires a large number of samples to converge. There is also a pertinent question of isolating the intermittency that is the result of turbulence dynamics from that of other kinematic effects, as occasionally posed in literature [4, 14, 15].

To address these concerns, in this letter, we ask the following questions: 1) What is a suitable baseline distribution, deviation from which is defined as turbulence intermittency? 2) Is there a more appropriate measure of intermittency that considers deviation of the complete PDF instead of a few select moments? For the former, we use a Gaussian random velocity field (GRF) as the baseline and define intermittency due to turbulence dynamics as the deviation from this baseline. For the latter, we turn to the information-theoretic measure of Kullback-Leibler (KL) divergence [16] that accounts for deviation

of the entire PDF and is robust to sampling errors in estimation [17–19]. KL divergence has previously been used to study transition in turbulent pipe flows [20], self-similarity and deviation from Gaussianity of the velocity field in turbulent boundary layers [21, 22], and inertial-range intermittency in grid turbulence and turbulent jets [23]. Here, we employ KL divergence to quantify small-scale intermittency as the deviation of an intermittent PDF of velocity-gradient quantities in turbulence from the corresponding baseline PDF.

Information-theoretic measures – Information theory is fundamentally based on the concept of Shannon entropy [24–26], which measures the uncertainty or information content of a random variable X as

$$H(X) = - \sum_{x \in \Pi_x} p(x) \log(p(x)) = - \int_{\Pi_x} f(x) \log(f(x)) dx - \log(\Delta x), \quad (1)$$

where $p(x)$ is the probability of a particular realization x of the random variable X (out of all possible realizations Π_x) and $f(x)$ is the corresponding PDF. Here, $p(x) \approx f(x)\Delta x$, for a finite, uniform spacing Δx between two consecutive realizations and Eq. (1) is valid under the assumptions of a small enough Δx and Riemann integrability of the integrand [27]. By definition, Shannon entropy is always non-negative. The logarithm in Eq. (1) and those throughout the manuscript are natural logarithms ($\log_e \equiv \ln$). Therefore, all entropy-based measures in this work are in units of nats.

Kullback-Leibler (KL) divergence or relative entropy of the PDF $f_1(x)$ of an intermittent random variable X , from the corresponding baseline PDF $f_2(x)$, is given by

$$D_{f_1||f_2}(X) = \int_{\Pi_x} f_1(x) \log\left(\frac{f_1(x)}{f_2(x)}\right) dx, \quad (2)$$

which is the amount of information lost when using $f_2(x)$ to represent $f_1(x)$ [16]. KL divergence is a non-negative asymmetric metric that measures the distance of the PDF $f_1(x)$ from the PDF $f_2(x)$, and vanishes only when

* rishitadas@iisc.ac.in

the two PDFs are identical. It quantifies the difference in the shapes of the two probability distributions, therefore, accounting for the contributions of all moments of X .

Measure of intermittency – To quantify small-scale intermittency, we evaluate how intermittent are the velocity gradient ($A_{ij} \equiv \partial u_i / \partial x_j$) quantities such as pseudodissipation rate ($\phi = A_{ij}A_{ij}$), dissipation rate ($\epsilon = S_{ij}S_{ij}$), and enstrophy ($\Omega = W_{ij}W_{ij}$) in a turbulent field compared to that in a Gaussian random velocity field. Here, $S_{ij} \equiv (A_{ij} + A_{ji})/2$ is the symmetric strain rate tensor and $W_{ij} \equiv (A_{ij} - A_{ji})/2$ is the skew-symmetric rotation rate tensor. The information-theoretic measures defined above are applied to mean-normalized fields $X/\langle X \rangle$ where $X = \phi, \epsilon$ or Ω . Hereafter, mean-normalized quantities $X/\langle X \rangle$ are denoted as X for simplicity.

To measure small-scale intermittency arising solely from turbulence dynamics, we compute the KL divergence, $D_{f||f_{GRF}}(X)$, of the PDF of X in a turbulent flow field, $f(x)$, from the PDF of X in a non-intermittent baseline field, $f_{GRF}(x)$. Next, we analytically derive the baseline distributions $f_{GRF}(x)$ for ϕ, ϵ and Ω .

Baseline Distribution – We consider a zero-mean divergence-free spatially-uncorrelated isotropic Gaussian random velocity field (GRF), as the non-intermittent baseline field. In such a field, the velocity gradient components (A_{ij}) are also Gaussian [28]. Consequently, the PDFs of mean-normalized pseudodissipation, dissipation, and enstrophy – being quadratic in A_{ij} – follow Gamma distributions, as shown by Gotoh and Yang [29]:

$$f_{GRF}(x) = \frac{\left(\frac{n}{2}\right)^{\frac{n}{2}}}{\Gamma\left(\frac{n}{2}\right)} x^{\frac{n}{2}-1} \exp\left(-\frac{nx}{2}\right), \quad (3)$$

where x is a probable realization of $X = \phi, \epsilon$ or Ω , and $\Gamma(\cdot)$ denotes gamma function. Here, n denotes the number of independent terms contributing to X , which is equal to 8, 5 and 3 for ϕ, ϵ and Ω , respectively, in a three-dimensional incompressible velocity field [29, 30]. Notably, the PDF is independent of the standard deviation of the velocity field due to the normalization by the mean. Consequently, the same baseline PDF can be used for evaluating intermittency of all Re_λ turbulent flows.

Expectedly, these Gamma PDFs of pseudodissipation, dissipation and enstrophy in the non-intermittent baseline field (Fig. 1) are significantly different from Gaussian, as measured by the KL divergence of these PDFs from Gaussian PDFs ($f_G(x)$) of same mean and variance,

$$D_{f_{GRF}||f_G}(X) = \log\left(\frac{\sqrt{n\pi}}{\Gamma\left(\frac{n}{2}\right)e^{\frac{n-1}{2}}}\right) + \left(\frac{n}{2} - 1\right) \psi\left(\frac{n}{2}\right) \quad (4)$$

which is equal to 0.08868, 0.14714 and 0.2607 for $X = \phi, \epsilon$ and Ω , where, $\psi(z) = (d\Gamma(z)/dz)/\Gamma(z)$ denotes the digamma function. The non-Gaussian nature of these quantities arises in a non-intermittent field because they are non-linear functions of the Gaussian velocity gradients and not because they possess intermittency from physical dynamics. This is referred to as kinematic intermittency [4, 14]. This questions the direct use of Gaus-

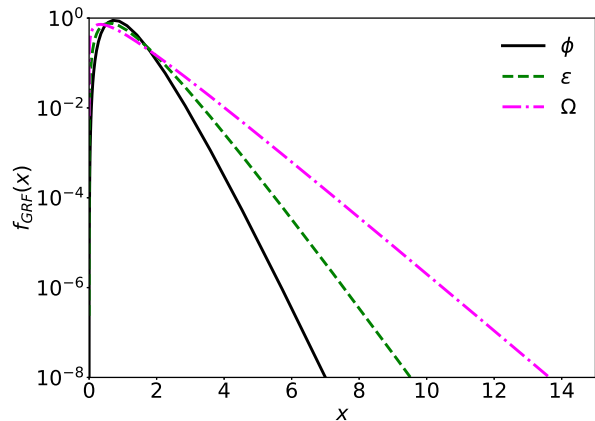


FIG. 1. PDF of baseline fields $f_{GRF}(X=x)$ for $X = \phi$ (pseudodissipation rate), ϵ (dissipation rate) and Ω (enstrophy) in log-linear scale.

sian PDF or moments as the baseline for assessing turbulence intermittency of ϕ, ϵ and Ω . Instead, the Gamma distributions (Eq. 3) of the GRF should be used as the baseline, deviation from which accurately measures intermittency due to turbulence dynamics.

Even in a non-intermittent GRF, Ω possesses a heavier-tailed PDF (Fig. 1) and thus, higher moments than ϵ . This is due to kinematic constraints in the definition of these quantities and shows that enstrophy has inherently greater kinematic intermittency than the dissipation rate [4, 14, 15]. Consequently, one can argue that heavier-tailed PDFs and higher moments in a turbulent field do not necessarily reflect stronger turbulence intermittency. Intermittency measured this way can be due to kinematic constraints and/or turbulence dynamics – the former is encoded in the baseline PDF, while the latter is quantified by the KL divergence from the baseline PDF. All subsequent references to intermittency in this work pertain to the turbulence-induced intermittency.

Direct Numerical Simulation (DNS) data – To study small-scale intermittency in turbulence, we analyze DNS data of forced homogeneous isotropic turbulence over a range of $Re_\lambda = 1$ to 588 in a periodic $(2\pi)^3$ domain. Two simulations of $Re_\lambda = 65$ and 121 are performed using an in-house pseudospectral solver [31], which treats the viscous term exactly and uses a linear forcing at low wavenumbers for maintaining statistical stationarity. It employs a low-storage second-order Runge-Kutta scheme for time integration [32], a parallel three-dimensional Fast Fourier Transform library [33], and the $2/3^rd$ -truncation rule for alias-free solutions [34]. Additionally, DNS datasets of forced isotropic turbulence obtained from the Johns Hopkins Turbulence Database and Donzis research group at Texas A&M University at $Re_\lambda = 1, 6, 9, 14, 18, 25, 35, 86, 225, 385, 427,$ and 588, are also used for analysis in this work [11, 35]. These datasets have been used in the past to study intermittency, scaling of high order moments, and velocity gradient dy-

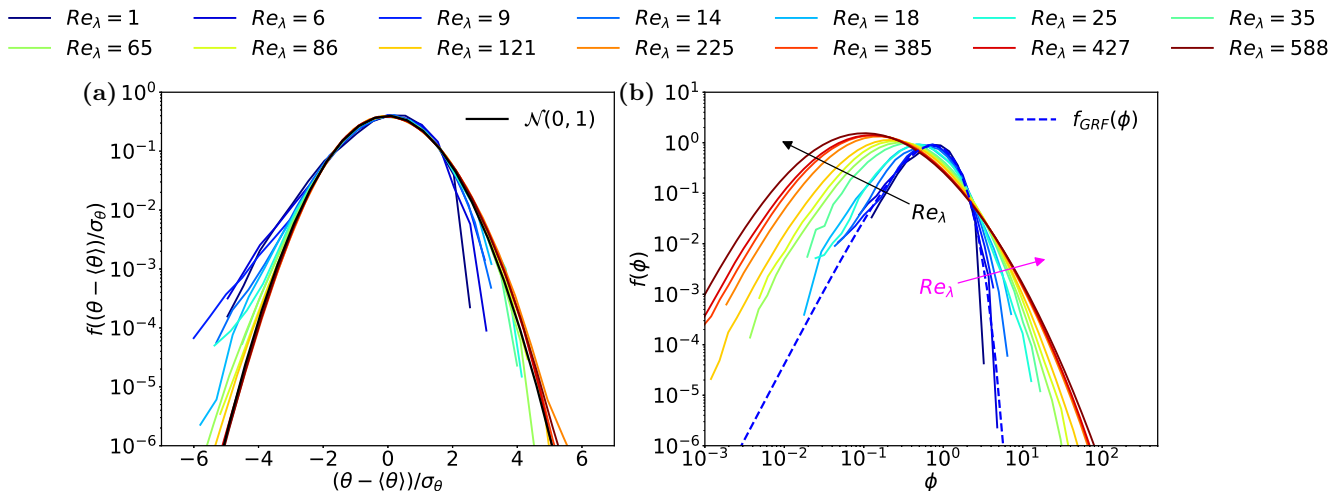


FIG. 2. (a) PDFs of standard normalized $\theta (\equiv \log(A_{ij}A_{ij}) = \log(\phi) + \log\langle A_{ij}A_{ij} \rangle)$ from DNS data of different Re_λ and standard normal fit $\mathcal{N}(0, 1)$ (black solid line). (b) PDFs of ϕ from DNS data of different Re_λ ($f(\phi)$) and from baseline field ($f_{GRF}(\phi)$, blue dashed line); arrows indicate the direction of increasing Re_λ .

namics [11, 36–39]. All DNS data are at resolutions: $k_{max}\eta \geq 1.32$, where k_{max} is the maximum resolved wave number normalized by the Kolmogorov length scale η . The PDFs are estimated from DNS data using the histogram method with the same bin width for all Re_λ , chosen based on convergence of KL divergence.

Lognormal distribution of pseudodissipation rate – We begin by examining the intermittency of pseudodissipation rate $\phi = A_{ij}A_{ij} / \langle A_{ij}A_{ij} \rangle$. At high enough Reynolds numbers, $A_{ij}A_{ij}$ follows a near-lognormal distribution [40, 41], implying that $\theta \equiv \log(A_{ij}A_{ij})$ is approximately Gaussian as shown in Fig. 2a. Therefore, the lognormal PDF fit for $\phi (= \exp(\theta) / \langle A_{ij}A_{ij} \rangle)$ can be derived as,

$$f_{fit}(\phi) = \frac{1}{\sqrt{2\pi}\sigma_\theta\phi} \exp \left[-\frac{1}{2\sigma_\theta^2} \left(\log(\phi) + \frac{1}{2}\sigma_\theta^2 \right)^2 \right]. \quad (5)$$

Note that $f_{fit}(\phi)$ only depends on one parameter – σ_θ (standard deviation of θ) that increases logarithmically with Re_λ : $\sigma_\theta^2 = -0.354 + 0.289 \log(Re_\lambda)$, as shown by Yeung & Pope [41] and Das & Girimaji [40] for $Re_\lambda \geq 10$. This lognormal PDF model will be used to verify and support the findings from DNS data.

Uncertainty – Shannon entropy or uncertainty (Eq. 1) of pseudodissipation rate, $H(\phi)$, is estimated from the DNS data and plotted as a function of Re_λ in Fig. 3. The variation of entropy with Reynolds number is further corroborated by that from the lognormal probability distribution, $H_{fit}(\phi)$ derived from Eqs. (1,5), for $Re_\lambda \geq 10$. For comparison, the figure also shows the entropy of ϕ in a non-intermittent Gaussian random velocity field, $H_{GRF}(\phi)$ obtained from Eqs. (1,3) [27]. There are two critical Reynolds numbers, $Re_\lambda^{(1)} \approx 10$ and $Re_\lambda^{(2)} \approx 100$, where the nature of uncertainty variation changes. Below $Re_\lambda^{(1)} \approx 10$, the entropy of pseudodissipation rate is close to that of a GRF, above which it has a more

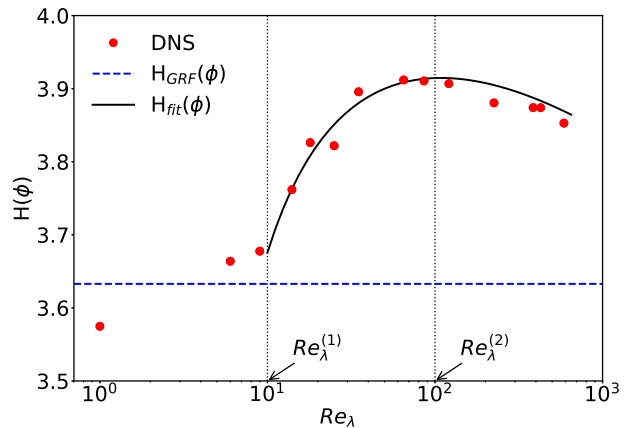


FIG. 3. Shannon entropy of pseudodissipation rate, $H(\phi)$, from DNS data of different Re_λ . Blue dashed line corresponds to the entropy in GRF, $H_{GRF}(\phi) \approx 0.637 - \log(\Delta x)$ and black solid line corresponds to the entropy from lognormal fit, $H_{fit}(\phi) = \log(\sqrt{2\pi}e/\Delta x) + \log(\sigma_\theta^2)/2 - \sigma_\theta^2/2$. Black dotted lines mark the two critical Reynolds numbers: $Re_\lambda^{(1)}$, $Re_\lambda^{(2)}$.

rapid growth in uncertainty as turbulence develops. At a similar transition Re_λ , velocity gradient moments begin to show deviation from Gaussianity [11, 12]. Hereafter, the variation of $H(\phi)$ with Re_λ can be explained by two competing effects in the PDF of ϕ (Fig. 2b) – entropy decreases as outcomes become less equiprobable (increase and narrowing of peak probability – black arrow) and entropy increases as more outcomes become possible (PDF tails widen – magenta arrow) [27, 29, 42]. In the range $Re_\lambda^{(1)} \leq Re_\lambda \leq Re_\lambda^{(2)}$, entropy increases due to the dominating effect of the stretching of the PDF tail and the growth in standard deviation, indicating the increasingly non-Gaussian nature of the flow. However,

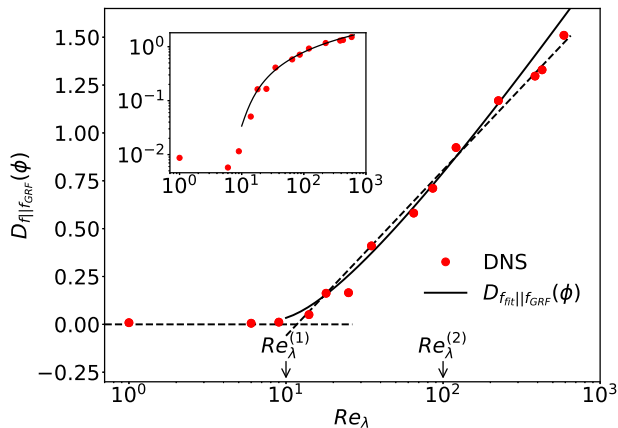


FIG. 4. KL divergence of turbulence pseudodissipation rate from baseline, $D_{f||f_{GRF}}(\phi)$, as a function of Re_λ in log-linear scale (log-log scale in inset). Dashed lines indicate: constant fit $D_{f||f_{GRF}}(\phi) \approx 0$ for $Re_\lambda \leq 10$ and log-law fit $D_{f||f_{GRF}}(\phi) \approx -0.925 + 0.376 \log(Re_\lambda)$ for $Re_\lambda \in (10, 600)$. Solid line indicates KL divergence obtained from the lognormal fit, $D_{f_{fit}||f_{GRF}}(\phi) = \log(3e^{7/2}/128\sqrt{2\pi}) + 2\sigma_\theta^2 - \frac{1}{2} \log \sigma_\theta^2$.

above $Re_\lambda^{(2)} \approx 100$, the entropy of ϕ decreases with further increase in Reynolds number, due to the dominating shape deformation of the PDF towards increased probability of very low- ϕ events. The critical $Re_\lambda^{(2)}$ is further validated by the lognormal fit, $H_{fit}(\phi)$, which attains its maximum at $\sigma_\theta^2 = 1 \implies Re_{\lambda_{fit}}^{(2)} = 108$. Interestingly, this is also the approximate Reynolds number at which specific small-scale statistics of turbulence converge, such as the normalized mean dissipation rate (dissipative anomaly) [43, 44], the average velocity-gradient partitioning into shear, normal-strain and rigid-body-rotation rates [38, 45], and the joint PDF of normalized second and third velocity-gradient invariants (q, r), representing the local streamline shape [46]. This suggests that the critical Reynolds number $Re_\lambda^{(2)}$ observed in the variation of entropy, potentially signifies the onset of fully developed turbulence, above which any further increase in Reynolds number leads to a more ordered state (and lower uncertainty) of small-scale turbulence.

Intermittency – Small-scale intermittency is typically studied by examining the moments of dissipation rate and enstrophy, that exhibit power-law scaling with Re_λ [36, 47–51]. For example, $\langle \Omega^n \rangle \sim Re_\lambda^{\beta_\Omega}$ where, each moment order n has a different scaling exponent, $\beta_\Omega = 0.42, 1.26, 2.28$ for $n = 2, 3, 4$ [51]. Quantifying intermittency using KL divergence integrates the effects of all these moments in one measure for each intermittent variable. Unlike moments, this measure isolates the intermittency arising solely from turbulence dynamics.

The KL divergence of pseudodissipation rate, $D_{f||f_{GRF}}(\phi)$, is plotted as a function of Re_λ in Fig. 4. At very low Reynolds numbers ($Re_\lambda \leq 10$), pseudodissipation rate exhibits nearly zero turbulence intermittency

and is close to a Gaussian random velocity field. The results indicate a transition at critical $Re_\lambda^{(1)} \approx 10$, above which $D_{f||f_{GRF}}(\phi)$ grows with Reynolds number, as the field deviates from GRF and becomes increasingly intermittent. This transitional behavior is consistent with that observed in the moments of longitudinal velocity gradients [12, 37]. After this transition, $D_{f||f_{GRF}}(\phi)$ increases logarithmically with Re_λ :

$$D_{f||f_{GRF}}(\phi) \approx -0.925 + 0.376 \log(Re_\lambda) \quad (6)$$

in the range $Re_\lambda \in (10, 600)$. The logarithmic growth of KL divergence indicates that the turbulence intermittency of ϕ increases with Re_λ but at a much slower rate than the power law scaling of the moments [11, 12]. The growth rate particularly slows down at high Re_λ (inset of Fig. 4) where the statistics of the small-scale structure of the turbulent field tend to converge [1, 38, 44–46]. The logarithmic growth is further supported by the approximate lognormal fit of ϕ , which yields a KL divergence of $D_{f_{fit}||f_{GRF}}(\phi) \sim 2\sigma_\theta^2 - \frac{1}{2} \log \sigma_\theta^2$, as derived from Eqs. (2,3,5). Since σ_θ^2 increases logarithmically with Re_λ , it follows that at high Re_λ , $\log(\sigma_\theta^2) \ll \sigma_\theta^2 \implies D_{f_{fit}||f_{GRF}}(\phi) \sim \sigma_\theta^2 \sim \log(Re_\lambda)$.

KL divergence of dissipation rate ϵ and enstrophy Ω follow a similar trend with Reynolds number as ϕ (Fig. 5). Below the same critical $Re_\lambda^{(1)} \approx 10$, both fields are nearly non-intermittent and follow the Gamma distribution of the baseline GRF in agreement with the findings of Gotou et al. [42]. Above $Re_\lambda^{(1)}$, both exhibit identical logarithmic growth in KL divergence, approximately:

$$D_{f||f_{GRF}}(X) \approx -0.46 + 0.17 \log(Re_\lambda), \quad X = \epsilon, \Omega. \quad (7)$$

Surprisingly, the intermittency of ϵ and Ω relative to their corresponding baseline distributions, are nearly identical to each other across all Reynolds numbers. This result is counterintuitive since Ω has traditionally been considered more intermittent than ϵ due to its elevated higher-order moments and heavier-tailed PDF [51–53]. However, these differences stem from kinematic intermittency, present even in non-intermittent Gaussian random velocity fields [4, 14, 54, 55], where $f_{GRF}(\Omega)$ inherently has a heavier tail than $f_{GRF}(\epsilon)$ (Fig. 1). Thus, our results suggest that turbulence dynamics induces nearly equal intermittency in both dissipation and enstrophy. Although unexpected, this finding aligns with prior observations: at high Re_λ , ϵ and Ω have nearly equal PDF-stretching exponents [36, 42], similar PDF shapes [56], comparable scaling exponents of moments [51], and Reynolds number collapse of PDFs when scaled by the same time scale [57]. Comparing Figs. 4 and 5, we further observe that pseudodissipation rate, despite being the least kinematically intermittent in a Gaussian random field (Fig. 1), exhibits greater intermittency due to turbulence dynamics than dissipation rate or enstrophy, and its intermittency grows more rapidly with Reynolds number.

Conclusion – This Letter introduces an information-theoretic framework to study small-scale intermittency

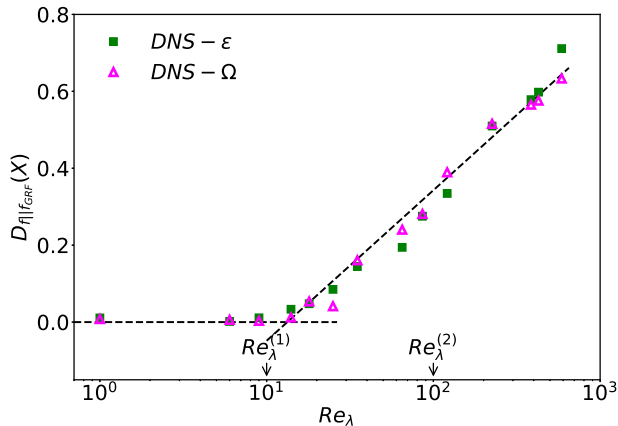


FIG. 5. KL divergence of dissipation rate $D_{f||f_{GRF}}(\epsilon)$ (green) and enstrophy $D_{f||f_{GRF}}(\Omega)$ (magenta) as a function of Re_λ . Dashed lines indicate: constant fit $D_{f||f_{GRF}}(X) \approx 0$ for $Re_\lambda \leq 10$ and log-law fit $D_{f||f_{GRF}}(X) \approx -0.46 + 0.17 \log(Re_\lambda)$ for $Re_\lambda \in (10, 600)$.

and uncertainty in turbulence. KL divergence of pseudodissipation, dissipation, and enstrophy of a homogeneous isotropic turbulent flow field with respect to that of a Gaussian random velocity field quantifies turbulence intermittency, excluding kinematic intermittency [4, 14, 42]. Analysis of DNS data reveals that contrary to prior findings, turbulence intermittency increases logarithmically with Reynolds number, and not as a power law. Remarkably, dissipation and enstrophy exhibit nearly equal turbulence intermittency, while pseu-

dodissipation exhibits the highest turbulence intermittency. The uncertainty (Shannon entropy) shows an unexpected trend - it grows at low Reynolds numbers potentially reflecting progressive symmetry breaking associated with the development of turbulence [58–61], but then it decays despite the increasing variability. This decay suggests a restoration of statistical symmetry at very high Reynolds numbers leading to a more ordered state of small-scale turbulence [62, 63]. Overall, the study identifies two critical Reynolds numbers: $Re_\lambda \approx 10$, where turbulence begins to emerge as the small scales become increasingly uncertain and intermittent with Reynolds number, and $Re_\lambda \approx 100$, above which small-scale structures are fully developed [43, 45, 46] and exhibit decreasing uncertainty and diminishing growth rate of intermittency. These findings offer a new quantitative understanding of small-scale intermittency in turbulence and the framework introduced here can be extended to study other intermittent physical systems.

Acknowledgments – The authors gratefully acknowledge the financial support provided by the United States Army Research Laboratory ITC-IPAC under contract no. FA520924C0025 and Indian Institute of Science for the Startup Research Grant of Rishita Das. The authors would like to thank the Donzis research group at Texas A&M University and Johns Hopkins Turbulence Database for providing part of the DNS data. The authors also acknowledge Mr. Aditya Prajapati and Mr. A. Bhargav Manohar for their help with the DNS solver. Computing resources of IISc Supercomputer Education and Research Centre (SERC) were used for numerical computations and data processing.

-
- [1] K. R. Sreenivasan and R. A. Antonia, The phenomenology of small-scale turbulence, *Annual Review of Fluid Mechanics* **29**, 435 (1997).
- [2] J. M. Lawson and J. R. Dawson, On velocity gradient dynamics and turbulent structure, *Journal of Fluid Mechanics* **780**, 60 (2015).
- [3] M. Wilczek and C. Meneveau, Pressure hessian and viscous contributions to velocity gradient statistics based on gaussian random fields, *Journal of Fluid Mechanics* **756**, 191 (2014).
- [4] A. Tsinober, *An Informal Conceptual Introduction to Turbulence*, Fluid Mechanics and Its Applications (Springer Netherlands, 2009).
- [5] E. D. Siggia, Numerical study of small-scale intermittency in three-dimensional turbulence, *Journal of Fluid Mechanics* **107**, 375 (1981).
- [6] D. Donzis and S. Sajeed, Degrees of freedom and the dynamics of fully developed turbulence, *Physical Review Fluids* **9**, 044605 (2024).
- [7] J. Schumacher, J. D. Scheel, D. Krasnov, D. A. Donzis, V. Yakhot, and K. R. Sreenivasan, Small-scale universality in fluid turbulence, *Proceedings of the National Academy of Sciences* **111**, 10961 (2014).
- [8] K. R. Sreenivasan and V. Yakhot, Dynamics of three-dimensional turbulence from navier-stokes equations, *Physical Review Fluids* **6**, 104604 (2021).
- [9] Y. Luo, Y. Shi, and C. Meneveau, Multifractality in a nested velocity gradient model for intermittent turbulence, *Physical Review Fluids* **7**, 014609 (2022).
- [10] T. Ishihara, Y. Kaneda, M. Yokokawa, K. Itakura, and A. Uno, Small-scale statistics in high-resolution direct numerical simulation of turbulence: Reynolds number dependence of one-point velocity gradient statistics, *Journal of Fluid Mechanics* **592**, 335 (2007).
- [11] V. Yakhot and D. A. Donzis, Multiscale dynamics and multiscaling in a random-force stirred fluid, *Phys. Rev. Lett.* **119**, 044501 (2017).
- [12] V. Yakhot and D. A. Donzis, Anomalous exponents in strong turbulence, *Physica D: Nonlinear Phenomena* **384-385**, 12 (2018).
- [13] J. Schumacher, K. R. Sreenivasan, and V. Yakhot, Asymptotic exponents from low-reynolds-number flows, *New Journal of Physics* **9**, 89 (2007).
- [14] A. Tsinober, J. Tsinober, and Jacobs, *Essence of turbulence as a physical phenomenon* (Springer, 2019).
- [15] L. Shtilman, M. Spector, and A. Tsinober, On some kinematic versus dynamic properties of homogeneous turbulence, *Journal of Fluid Mechanics* **247**, 65 (1993).

- [16] S. Kullback, *Information Theory and Statistics*, Dover Books on Mathematics (Dover Publications, 2012).
- [17] F. Bovolo and L. Bruzzone, An adaptive technique based on similarity measures for change detection in very high resolution sar images, in *IGARSS 2008-2008 IEEE International Geoscience and Remote Sensing Symposium*, Vol. 3 (IEEE, 2008) pp. III–158.
- [18] S. Jabari, M. Rezaee, F. Fathollahi, and Y. Zhang, Multispectral change detection using multivariate kullback-leibler distance, *ISPRS Journal of Photogrammetry and Remote Sensing* **147**, 163–179 (2019).
- [19] D. D. Saurette, R. J. Heck, A. W. Gillespie, A. A. Berg, and A. Biswas, Divergence metrics for determining optimal training sample size in digital soil mapping, *Geoderma* **436**, 116553 (2023).
- [20] R. Raj, A. Thiruthummal, and A. Potherat, Detecting turbulent patterns in particulate pipe flow by streak angle visualization, arXiv preprint arXiv:2501.01753 (2025).
- [21] A. Zhou and J. Klewicki, Properties of the streamwise velocity fluctuations in the inertial layer of turbulent boundary layers and their connection to self-similar mean dynamics, *International Journal of Heat and Fluid Flow* **51**, 372 (2015).
- [22] Y. Tsuji and I. Nakamura, Probability density function in the log-law region of low reynolds number turbulent boundary layer, *Physics of Fluids* **11**, 647 (1999).
- [23] C. Granero-Belinchón, S. G. Roux, and N. B. Garnier, Kullback-leibler divergence measure of intermittency: Application to turbulence, *Phys. Rev. E* **97**, 013107 (2018).
- [24] C. E. Shannon, A mathematical theory of communication, *The Bell System Technical Journal* **27**, 379 (1948).
- [25] A. Y. Khinchin, *Mathematical foundations of information theory* (Courier Corporation, 2013).
- [26] A. Lesne, Shannon entropy: a rigorous notion at the crossroads between probability, information theory, dynamical systems and statistical physics, *Mathematical Structures in Computer Science* **24**, e240311 (2014).
- [27] T. Cover and J. Thomas, *Elements of Information Theory* (Wiley, 2012).
- [28] E. Solak, R. Murray-Smith, W. Leithead, D. Leith, and C. Rasmussen, Derivative observations in gaussian process models of dynamic systems, *Advances in neural information processing systems* **15** (2002).
- [29] T. Gotoh and J. Yang, Transition of fluctuations from gaussian state to turbulent state, *Mathematical Physics and Engineering Sciences* **380**, 2021007 (2022).
- [30] C. Meneveau, Lagrangian dynamics and models of the velocity gradient tensor in turbulent flows, *Annual Review of Fluid Mechanics* **43**, 219 (2011).
- [31] R. Rogallo, *Numerical Experiments in Homogeneous Turbulence*, NASA technical memorandum, Vol. 81315 (National Aeronautics and Space Administration, 1981).
- [32] C. Canuto, M. Hussaini, A. Quarteroni, and J. Thomas A., *Spectral Methods in Fluid Dynamics*, Scientific Computation (Springer Berlin Heidelberg, 2012).
- [33] D. Pekurovsky, P3dffft: A framework for parallel computations of fourier transforms in three dimensions, *SIAM Journal on Scientific Computing* **34**, C192 (2012).
- [34] S. A. Orszag and G. S. Patterson, Numerical simulation of three-dimensional homogeneous isotropic turbulence, *Phys. Rev. Lett.* **28**, 76 (1972).
- [35] Y. Li, E. Perlman, M. Wan, Y. Yang, C. Meneveau, R. Burns, S. Chen, A. Szalay, and G. Eyink, A public turbulence database cluster and applications to study lagrangian evolution of velocity increments in turbulence, *Journal of Turbulence* **9**, N31 (2008).
- [36] D. A. Donzis, P. K. Yeung, and K. R. Sreenivasan, Dissipation and enstrophy in isotropic turbulence: Resolution effects and scaling in direct numerical simulations, *Physics of Fluids* **20**, 045108 (2008).
- [37] R. Das and S. S. Girimaji, On the reynolds number dependence of velocity-gradient structure and dynamics, *Journal of Fluid Mechanics* **861**, 163–179 (2019).
- [38] R. Das and S. S. Girimaji, Revisiting turbulence small-scale behavior using velocity gradient triple decomposition, *New Journal of Physics* **22**, 063015 (2020).
- [39] Y. Lin and H. Xu, Experimental investigation of pressure statistics in laboratory homogeneous isotropic turbulence, *Physics of Fluids* **35** (2023).
- [40] R. Das and S. S. Girimaji, Data-driven model for lagrangian evolution of velocity gradients in incompressible turbulent flows, *Journal of Fluid Mechanics* **984**, A39 (2024).
- [41] P. K. Yeung and S. B. Pope, Lagrangian statistics from direct numerical simulations of isotropic turbulence, *Journal of Fluid Mechanics* **207**, 531–586 (1989).
- [42] T. Gotoh, T. Watanabe, and I. Saito, Kinematic effects on probability density functions of energy dissipation rate and enstrophy in turbulence, *Phys. Rev. Lett.* **130**, 254001 (2023).
- [43] K. R. Sreenivasan, An update on the energy dissipation rate in isotropic turbulence, *Physics of Fluids* **10**, 528 (1998).
- [44] D. Donzis, K. Sreenivasan, and P. K. Yeung, Scalar dissipation rate and dissipative anomaly in isotropic turbulence, *Journal of Fluid Mechanics* **532**, 199 (2005).
- [45] R. Arun and T. Colonius, Velocity gradient partitioning in turbulent flows, *Journal of Fluid Mechanics* **1000**, R5 (2024).
- [46] R. Das and S. S. Girimaji, The effect of large-scale forcing on small-scale dynamics of incompressible turbulence, *Journal of Fluid Mechanics* **941**, A34 (2022).
- [47] T. Zhou and R. Antonia, Reynolds number dependence of the small-scale structure of grid turbulence, *Journal of Fluid Mechanics* **406**, 81 (2000).
- [48] A. Vela-Martín, The energy cascade as the origin of intense events in small-scale turbulence, *Journal of Fluid Mechanics* **937**, A13 (2022).
- [49] S. K. Yeung and K. R. Sreenivasan, Scaling and universality of universal scaling in isotropic turbulence, *Physical Review E* **107**, 045102 (2023).
- [50] D. Buaria and K. R. Sreenivasan, Scaling of acceleration statistics in high reynolds number turbulence, *Physical Review Letters* **128**, 234502 (2022).
- [51] G. Elsinga, T. Ishihara, and J. Hunt, Intermittency across reynolds numbers – the influence of large-scale shear layers on the scaling of the enstrophy and dissipation in homogenous isotropic turbulence, *Journal of Fluid Mechanics* **974**, A17 (2023).
- [52] S. Chen, K. R. Sreenivasan, and M. Nelkin, Inertial range scalings of dissipation and enstrophy in isotropic turbulence, *Physical review letters* **79**, 1253 (1997).
- [53] D. Buaria, A. Pumir, E. Bodenschatz, and P.-K. Yeung, Extreme velocity gradients in turbulent flows, *New Journal of Physics* **21**, 043004 (2019).

- [54] S. Chen, G. D. Doolen, R. H. Kraichnan, and L.-P. Wang, Is the kolmogorov refined similarity relation dynamic or kinematic?, *Physical review letters* **74**, 1755 (1995).
- [55] H. Chen and S. Chen, Kinematic effects on local energy dissipation rate and local enstrophy in fluid turbulence, *Physics of Fluids* **10**, 312 (1998).
- [56] P. Yeung, K. Sreenivasan, and S. Pope, Effects of finite spatial and temporal resolution in direct numerical simulations of incompressible isotropic turbulence, *Physical Review Fluids* **3**, 064603 (2018).
- [57] D. Buaria and A. Pumir, Vorticity-strain rate dynamics and the smallest scales of turbulence, *Physical Review Letters* **128**, 094501 (2022).
- [58] U. Frisch and A. N. Kolmogorov, *Turbulence: the legacy of AN Kolmogorov* (Cambridge university press, 1995).
- [59] E. Bormashenko, I. Legchenkova, and M. Frenkel, Symmetry and shannon measure of ordering: Paradoxes of voronoi tessellation, *Entropy* **21**, 452 (2019).
- [60] E. Bormashenko, Entropy, information, and symmetry: Ordered is symmetrical, *Entropy* **22**, 11 (2019).
- [61] E. Bormashenko, Entropy, information, and symmetry; ordered is symmetrical, ii: system of spins in the magnetic field, *Entropy* **22**, 235 (2020).
- [62] Z. Warhaft, Turbulence in nature and in the laboratory, *Proceedings of the National Academy of Sciences* **99**, 2481 (2002).
- [63] N. Antonov, N. Gulitskiy, M. Kostenko, and A. Malyshov, Statistical symmetry restoration in fully developed turbulence: Renormalization group analysis of two models, *Physical Review E* **97**, 033101 (2018).